

High-Resolution Structural Analysis Shows How Tah1 Tethers Hsp90 to the R2TP Complex

Régis Back,^{1,5} Cyril Dominguez,^{2,6} Benjamin Rothé,^{1,7} Claude Beaufils,³ Solange Moréra,⁴ Philippe Meyer,^{4,8} Bruno Charpentier,¹ Christiane Branlant,¹ Frédéric H.-T. Allain,^{2,*} and Xavier Manival^{1,*}

¹Ingénierie Moléculaire et Physiopathologie Articulaire (IMoPA), UMR 7365 Université de Lorraine-CNRS, Biopôle de l'Université de Lorraine, Campus Biologie Santé, 9 Avenue de la forêt de Haye, BP 184, 54505 Vandœuvre-lès-Nancy, France

²Institute of Molecular Biology and Biophysics (IMB), ETH Zurich, CH-8093 Zurich, Switzerland

³LCPM, Groupe Synthèse Organique et Biostructures, UMR CNRS-INPL 7568, 1, rue Grandville, BP 20451, F-54001 Nancy Cedex, France

⁴Laboratoire d'Enzymologie et Biochimie Structurales (LEBS), UPR CNRS 3082, Bât. 34, 91198 Gif-sur-Yvette Cedex, France

⁵Present address: Laboratoire de Biochimie, CNRS UMR7654, Ecole Polytechnique, Route de Saclay, 91128 Palaiseau, France

⁶Present address: Department of Biochemistry, University of Leicester, LE1 9HN Leicester, UK

⁷Present address: Ecole Polytechnique Fédérale de Lausanne (EPFL), School of Life Sciences - ISREC, CH-1015 Lausanne, Switzerland

⁸Present address: Laboratoire de Biologie Moléculaire et Cellulaire des Eucaryotes - Institut de Biologie Physico-Chimique, CNRS-UPMC, 15 rue Pierre et Marie Curie 75005 Paris, France

*Correspondence: allain@mol.biol.ethz.ch (F.H.-T.A.), xavier.manival@univ-lorraine.fr (X.M.)

<http://dx.doi.org/10.1016/j.str.2013.07.024>

SUMMARY

The ubiquitous Hsp90 chaperone participates in snoRNP and RNA polymerase assembly through interaction with the R2TP complex. This complex includes the proteins Tah1, Pih1, Rvb1, and Rvb2. Tah1 bridges Hsp90 to R2TP. Its minimal TPR domain includes two TPR motifs and a capping helix. We established the high-resolution solution structures of Tah1 free and in complex with the Hsp90 C-terminal peptide. The TPR fold is similar in the free and bound forms and we show experimentally that in addition to its solvating/stabilizing role, the capping helix is essential for the recognition of the Hsp90⁷⁰⁴EMEEVD⁷⁰⁹ motif. In addition to Lys79 and Arg83 from the carboxylate clamp, this helix bears Tyr82 forming a π/S-CH3 interaction with Hsp90 M⁷⁰⁵ from the peptide 3₁₀ helix. The Tah1 C-terminal region is unfolded, and we demonstrate that it is essential for the recruitment of the Pih1 C-terminal domain and folds upon binding.

INTRODUCTION

The highly conserved eukaryotic Hsp90 (90-kDa heat-shock protein) is an essential ubiquitous ATP-dependent molecular chaperone. In addition to its activity as a chaperone protein in stress conditions, Hsp90 is required for conformational maturation of signal transduction proteins and is therefore linked to cell cycle regulation and cancer progression (reviewed in Whitesell and Lin, 2012). Hsp90 specifically recognizes a set of protein substrates, designated as client proteins, such as transcription factors, protein kinases, and hTERT (Theodoraki and Caplan, 2012). In addition, Hsp90 was recently shown to play a crucial role in the assembly of several essential eukaryotic ubiquitous cellular machineries. They include (1) ribonucleoprotein particles

(RNPs), namely the box C/D and box H/ACA snoRNPs that respectively guide and catalyze 2'-O methylations and pseudouridylations in preribosomal RNA, the spliceosomal U4 snRNP, the telomerase RNP, and selenoprotein mRNPs (Boulon et al., 2008; Zhao et al., 2008); (2) the nuclear RNA polymerases (Boulon et al., 2010), and (3) the phosphatidylinositol 3-kinase-related protein kinase family, including proteins mTOR and SMG1 (Horejsí et al., 2010). How Hsp90 is involved in these highly important functions has still to be deciphered.

Hsp90 reveals the activity of its client proteins by acting when they are in a near-native state (reviewed in Pearl and Prodromou, 2006). Hsp90 is also involved in the degradation of trapped misfolded proteins via the ubiquitin-proteasome pathway (Connell et al., 2001). The Hsp90 chaperone activity depends on the ATPase activity carried by its N-terminal and middle domains (Meyer et al., 2003b), and inhibition of this activity by geldanamycin blocks cell proliferation (Whitesell and Cook, 1996). Interestingly, geldanamycin was also shown to block the recently discovered functions of Hsp90 in the snoRNP and RNA polymerase assembly (Boulon et al., 2008; Boulon et al., 2010; Zhao et al., 2008). The Hsp90 C-terminal domain is responsible for Hsp90 dimerization. In its dimeric form, Hsp90 acts as a molecular clamp whose transient closure allows ATP hydrolysis (Ali et al., 2006).

To achieve its protein maturation activity, Hsp90 cooperates with another molecular chaperone, Hsp70, and numerous cofactors called cochaperones. Through modulation of ATP binding or hydrolysis, these cochaperones participate in the regulation of the Hsp90 ATPase cycle (reviewed in Prodromou, 2012), and in the specific recognition of protein substrates (reviewed in Li et al., 2012). Many Hsp90/70 co-chaperones contain tetratrico-peptide repeat domains (TPR domains) and/or aspartate- and proline-rich domains (DP domains; Nelson et al., 2003). These proteins bind to the 20-amino acid C-terminal sequence of Hsp90 that contains the conserved MEEVD motif (reviewed in Zeytuni and Zarivach, 2012).

The crystal structures established for the Hsp90 or Hsp70 C-terminal domain in complex with partner TPRs brought information on determinants ensuring TPR recognition (Scheufler

Structure

NMR Structures of Tah1 and Its Complex with Hsp90

et al., 2000). For instance, Hsp70 and Hsp90 recognize distinct TPR domains in the Hop (HSP-organizing protein) cofactor (TPR1 and TPR2A, respectively). TPR domains contain 3 to 16 TPR motifs (reviewed in Zeytuni and Zarivach, 2012) that are defined by a 34-amino acid element organized into a common helix-turn-helix structure with only a few conserved residues. The TPR domains of the Hsp70/90 cochaperones share five exposed residues that form the dicarboxylate clamp interacting with the aspartic acid of the Hsp70 and Hsp90 EEVD motifs (Russell et al., 1999; Scheufler et al., 2000). Discrimination between Hsp90 and Hsp70 by the cochaperones depends on the identity of the amino acid located upstream of the EEVD element, a methionine residue, and an isoleucine residue, respectively (Scheufler et al., 2000). Recently, Schmid and colleagues solved the nuclear magnetic resonance (NMR) structures of the two DP domains of the Hsp90 co-chaperone Sti1/Hop and showed that DP2 is required for client activation in vivo (Schmid et al., 2012).

To ensure its recently discovered functions in the assembly of macromolecules, Hsp90 associates with one peculiar cochaperone complex, the R2TP. In yeast this complex contains the two AAA+ ATPases/helicases Rvb1 and Rvb2 and the proteins Pih1 (protein interacting with Hsp90) and Tah1 (TPR containing protein associated with Hsp90). The four vertebrate counterpart proteins are TIP49, TIP48, PIH1D1, and RPAP3 (Boulon et al., 2008). Pih1 contains two domains including a CS domain at the C terminus (Finn et al., 2010). This protein is necessary for nucleolar retention of the box C/D core proteins in *Saccharomyces cerevisiae* (Gonzales et al., 2005). Pih1 forms a stable complex with Tah1 that downregulates the Hsp90 ATPase activity (Eckert et al., 2010). Tah1 contains two TPR motifs (Zhao et al., 2008) that share sequence similarity with the Hop TPR2B domain (this third Hop TPR domain has no identified high-affinity ligand; Millson et al., 2008; Scheufler et al., 2000).

Determining how Tah1 interacts with Hsp90 is essential to explain how Tah1 tethers Hsp90 to the R2TP complex. Recently, the structure of Tah1 in complex with the MEEVD peptide corresponding to the yeast Hsp90 C terminus was studied with NMR (Jiménez et al., 2012). However, due to the low number of intermolecular NOE restraints, the structure of the bound Hsp90 peptide was modeled. Consequently, the resolution of the proposed structure is not sufficient to fully understand the specificity of complex formation.

Here, we report the high-resolution structures of both free Tah1 and Tah1 bound to the ADTEMEEVD C-terminal sequence of Hsp90 established with a large panel of NMR approaches. Our data highlight how the Hsp90 terminal peptide is bound to Tah1 and explain the specificity of the interaction. We also describe *in vitro* and *in cellulo* analyses of the Tah1:Hsp90 and Tah1:Pih1 interactions. Altogether, our data bring important information on how Hsp90 recognizes the R2TP complex.

RESULTS

Free Tah1 NMR Structure Reveals a Short TPR Domain Flanked by a Flexible C-Terminal Region

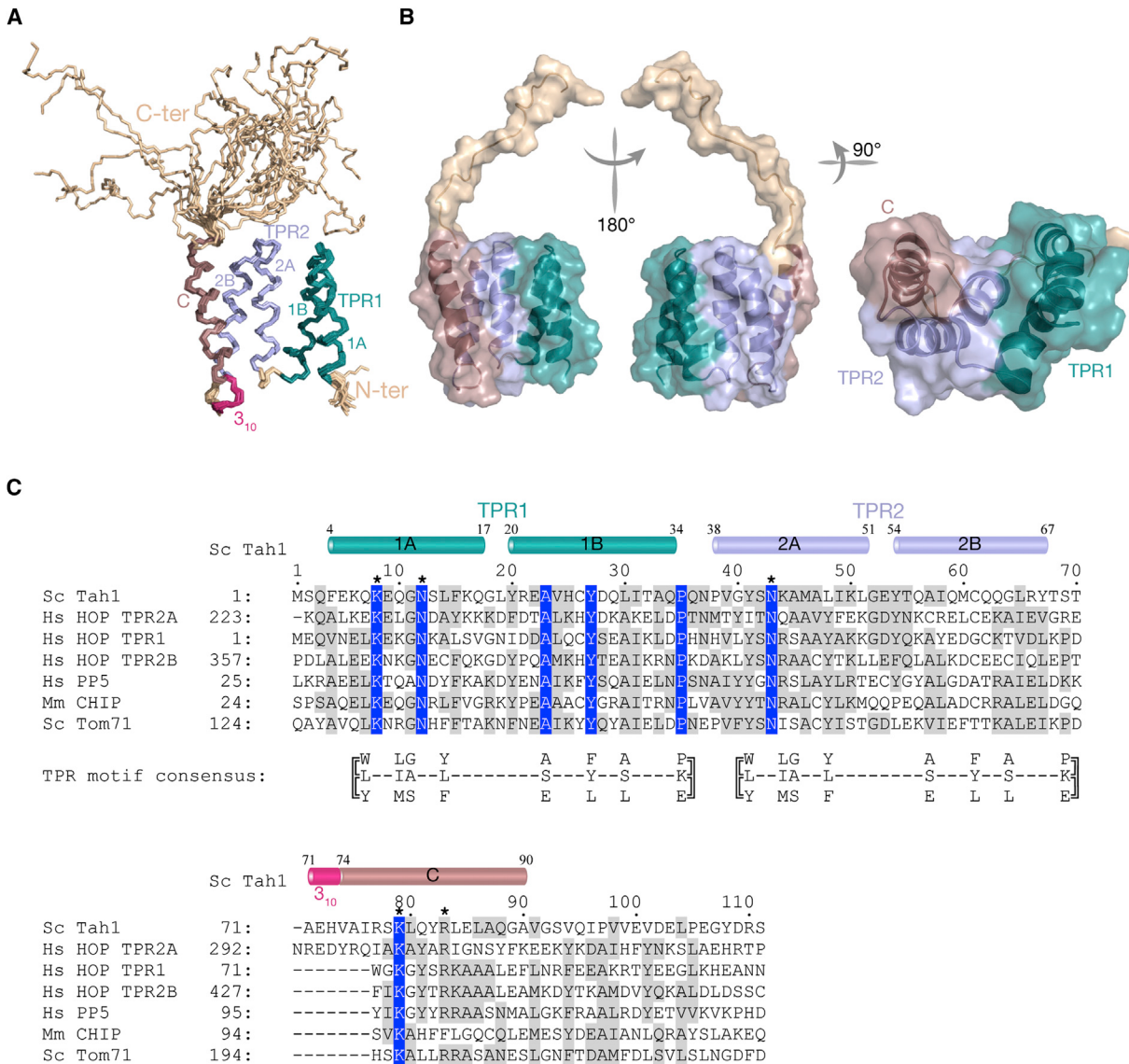
To study the structure of the free Tah1 protein in solution using NMR, we produced a ¹⁵N-¹³C-labeled Tah1 protein. Backbone and side chain resonance were assigned using conventional methods (Sattler et al., 1999). Structure calculations based on

NOESY spectra were performed using CYANA (Güntert, 2004), followed by refinement with AMBER (Case et al., 2005). Figure 1 shows the superposition of the 20 conformers with the lowest energy that best satisfies the experimental restraints (Figures 1A and 1B). This family of 20 conformers is well defined with a root-mean-square deviation (rmsd) for the backbone atoms of the 4–90 amino acid stretch of 0.44 ± 0.08 Å (Table 1). The data reveal the presence of a structured N-terminal TPR domain (1–92) flanked by a flexible short C-terminal region (93–111). As expected from previous predictions (Millson et al., 2008; Zhao et al., 2008), the N-terminal residues (1–67) are folded into two tandem TPR motifs (TPR1 and TPR2), each composed of a pair of antiparallel α helices: amino acid stretches 4–17 and 20–34 for TPR1, and amino acids stretches 38–51 and 54–67 for TPR2 (Figure 1). The Tah1 TPR1 contains the highly conserved TPR residues Gly/Ala11, Ala23, Tyr27, Pro35, and the less conserved residues Leu14 and Leu30 (reviewed in Zeytuni and Zarivach, 2012). The Tah1 TPR2 is more degenerated (Figure 1C). It contains only one of the conserved TPR residues, Asn43, which is part of the dicarboxylate clamp. The interhelical angles in the TPR1 and TPR2 motifs range from 155° to 168° according to MOLMOL software calculations (Koradi et al., 1996). They are highly similar to those calculated for other Hsp cochaperones. Helix 2B in TPR2 is tightly associated through hydrophobic contacts with a fifth helix (residues 74–90), designated as capping helix or helix C (Das et al., 1998). These contacts involve on one hand Leu84 and Val91 of helix C and Ile58 of TPR2, and on the other hand, Leu80 in helix C and Leu65 of TPR2 (Figure S1A available online). Helix C does not display the sequence hallmarks of the first helix of a third TPR motif. However, it bears the conserved Lys79 and Arg83 residues that participate in carboxylate clamp formation (Figure 1C). The angle defined by helix C and helix 2B is small (145°) compared to angles in TPR motifs. Therefore, in free Tah1, helix C can be considered as the capping/solubilizing helix of the short Tah1 TPR domain. As usual, the two helices of each TPR motif interact through their hydrophobic face, while their opposite hydrophilic faces are exposed to the solvent (reviewed in Zeytuni and Zarivach, 2012). The additional amphipathic helix C fully participates in the formation of a compact helix-turn-helix arrangement, which is characteristic of TPR domains (Figure 1C). Lastly, a β_{10} helix encompassing residues 71–73 was detected in some but not all the 20 structures of lowest energy (Figure 1A).

The 19-amino acid C-terminal region (positions 93–111) located immediately downstream from helix C displays the characteristic features of an unstructured region, with random coil chemical shifts and reduced ¹H-¹⁵N heteronuclear NOE values indicative of elevated motion relative to the TPR domain (Figure S2A). Interestingly, the surface of the N-terminal domain is predominantly positive, while the C-terminal region is negatively charged (Figure S2B), suggesting distinct protein binding properties for these two regions.

The N and C Regions of Tah1 Interact with Different Protein Partners

In the R2TP-Hsp90 complex, Tah1 is bound to both Pih1 and Hsp90 (Zhao et al., 2005). Although, the Tah1 N-terminal TPR domain was expected to bind Hsp90, a recombinant protein containing the TPR1 and TPR2 motifs but not helix C failed to

**Figure 1. The Solution NMR Structure of Free Tah1**

(A) Backbone view of the 20 energetically lowest conformers of free Tah1 with representation of TPR1 (turquoise), TPR2 (gray), helix C (brown), and helix 3₁₀ (red). This color code is used in all figures of this manuscript.

(B) PyMOL transparent surface orthogonal views of the free Tah1 energetically lowest conformer with inside ribbon representation of the protein chain (DeLano, 2010).

(C) Structure-based sequence alignment of various TPR domains of eukaryotic Hsp70/90 cochaperones. The GenBank sequences of Hsp70-binding TPR domains: Hop-TPR1 (P31948) and CHIP (Q9WUD1); and Hsp90-binding TPR domains: Hop-TPR2A (P31948), Hop-TPR2B (P31948), PP5 (P53041), Tah1 (P25638), and Tom71 (P38825) from *Homo sapiens* (Hs), *Mouse musculus* (Mm), or *S. cerevisiae* (Sc) were aligned using CLUSTAL W and optimized manually. Amino acid numbering is that of Tah1. Identical residues are highlighted in blue rectangles. Residues exhibiting more than 50% of conservation are in gray boxes. Residues implicated in the carboxylate clamp are marked by stars above the Tah1 sequence. The TPR consensus sequence (below the sequences) is aligned with the Tah1 TPR1 and TPR2 sequences. Secondary structure elements are represented at the top with the color code used in (A). See also Figures S1 and S2.

interact with Hsp90 (Zhao et al., 2008). Having delineated a short TPR domain (two TPR motifs + helix C) and a flexible C-terminal region in free Tah1, we used yeast two-hybrid assays (Y2H; Figure 2A) to test their respective capacities to bind to Hsp90 and Pih1 in cellulo. To this end, the nucleotide sequences encoding (1) full-length Tah1, (2) the C-terminal region, and (3) the short TPR domain were individually cloned into the Y2H plasmid

pGBKT7 and the nucleotide sequences encoding Pih1 and Hsp90 were inserted into the Y2H plasmid pACTII. Various concentrations of 3-amino-1,2,4-triazol (3AT) were used to evaluate the strength of the interactions in yeast cells (Figure 2A). In these assays, the full-length Tah1 and the short TPR domain were both found to establish tight (stable at 10 mM 3AT) interactions with Hsp90, strongly indicating that the short TPR domain

Table 1. NMR Structure determination statistics of the tah1 protein and Tah1-yeast Hsp90 complex

	Free form	Complex		
	Tah1 protein	Tah1 protein	Tah1:Hsp90	Yeast Hsp90 peptide
NMR distance constraints				
Total Intramolecular Noes	1786	2659		56
Intra-residue	482	610		19
Inter-residues				
Sequential	448	687		25
Medium range	411	776		12
Long range	445	586		0
Total Intermolecular Noes			55	
Structure statistics				
RMSD to mean structure				
Backbone atoms	0.44 ± 0.08 ^a	0.36 ± 0.10 ^a	0.42 ± 0.10 ^{a,b}	0.56 ± 0.21 ^b
Heavy atoms	0.98 ± 0.13 ^a	0.86 ± 0.12 ^a	0.92 ± 0.12 ^{a,b}	1.30 ± 0.25 ^b
RMSD from idealized covalent geometry				
Bond length (Å)	0.0038 ± 0.0001		0.0042 ± 0.0001	
Bond angle (°)	1.43 ± 0.02		1.74 ± 0.03	
Violations				
Average number of violations (>0.4 Å)	0.00		9.6	
Highest violation (Å)	0.39		0.95	
Energies (kcal.mol ⁻¹)				
Average AMBER	−4009 ± 20		−4146 ± 17.5	
Average constraint violations energy	96 ± 10		530 ± 18	
Ramachandran analysis				
Most favored	70.6		74.8	
Additionally allowed region	28.3		22.9	
Generously allowed region	1.0		2.1	
Disallowed region	0.1		0.2	

^ar.m.s. deviation was calculated using residues 4–90 for the ensemble of 20 refined structures.

^br.m.s. deviation was calculated using residues 704–709 for the ensemble of 20 refined structures.

represents the Hsp90 recognition domain of Tah1. This domain did not interact with Pih1 in the assays, while the isolated C-terminal region did (Figure 2A). Therefore, in Y2H assays, the short unstructured C-terminal region of Tah1 was sufficient to bind Pih1 and the strength of the interaction was similar to that for full-length Tah1.

The 253–344 C-Terminal Fragment of Pih1 Interacts with the Tah1 C-Terminal Region

Mass spectrometry analysis showed that the Pih1 fragment extending from position 199 to 344 binds to Tah1 in vitro (Eckert et al., 2010). To further delineate the Tah1 binding site in Pih1, we again used Y2H assays. Alignment of the yeast and human Pih1 amino acid sequences revealed an inserted 42 amino acid sequence in yeast Pih1 that separates (1) the N-terminal 211 amino acid sequence showing 38% similarity in the two proteins and (2) the 92 C-terminal amino acid sequence displaying 24% of similarity in the two proteins (Figure 2B). The Pih1(1–252) N-terminal region, which includes the yeast-specific sequence, did not interact with Tah1 in Y2H assays, while an efficient interaction was detected with the Pih1(253–344) C-terminal region (Figure 2B). Therefore, our data indicated that the 92 C-terminal amino acids of Pih1 are sufficient for association with Tah1 in vivo.

To test whether this interaction is direct, we produced a ¹⁵N-labeled His₆-Tah1:Pih1 (257–344) complex in *E. coli* by coexpression. Because Pih1 produced alone in *E. coli* is unstable, we could not get individual ¹⁵N labeling of each protein in the complex. Retention of the complex on cobalt-sepharose beads after cell lysis and its purification after 3C cleavage by gel filtration brought strong evidence for a direct interaction between the two proteins (data not shown). In addition, superposition of the (¹⁵N-¹H) heteronuclear single-quantum coherence (HSQC) spectrum of free Tah1 with that of the complex (red and black, respectively, in Figure 3) showed that the NH peaks of the TPR domain (1–90) are not modified upon addition of the Pih1 fragment (see the zooms for residues G11, R21, H25, D28, A33, Q34, N37, A47, E53, Y67, and L80), while the NH peaks of the free and bound C-terminal part of Tah1 (91–111) do not overlap (see the zooms for residues V91, G92, S93, E100, and G107). The additional peaks observed at the bottom of the spectrum (black ones around 9 ppm in Figure 3) mainly correspond to the bound residues of Pih1(257–344). Additional signals in bound Pih1 are not in favor of large random coil regions. Further analyses are underway to solve the structure of the complex. However, HSQC data strongly reinforced the idea that fragment 257–344 of Pih1 interacts directly with the 19 most C-terminal amino acids of Tah1.

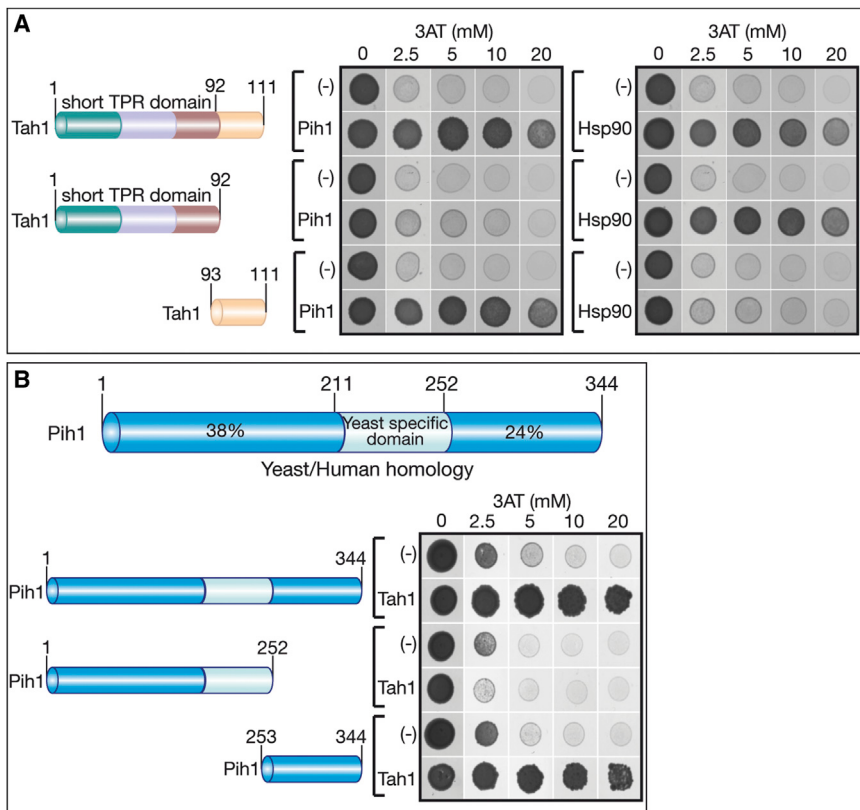


Figure 2. In Cellulo Mapping of the Tah1:Pih1 and Tah1:Hsp90 Interactions

(A) Yeast 2H tests of the Pih1 and Hsp90 interactions with full length Tah1, the Tah1 TPR domain and its unfolded C-terminal fragment. Tah1 and its fragments (same color code as in Figure 1) were used as baits (pGKTK7-Gal4BD) and Pih1 (left picture) or Hsp90 (right picture) as the prey (pACTII-Gal4AD). Empty pACTII plasmid (-) was used as a negative control. Strains Y190 and Y187 are auxotrophic for histidine. Activation of the *HIS3* reporter gene by interaction between the bait and prey is needed for growth. Similar growths at high 3-amino-1,2,4-triazole (3AT) (a competitive inhibitor of the *HIS3* gene product) concentrations indicate that full-length Tah1 and the Tah1 C-terminal fragment have similar in cel-lulo affinities for Pih1.

(B) Y2H tests for in cellulo interactions of full length Pih1 and Pih1 1–252 and 253–344 domains with Tah1. Pih1 and its fragments were the baits (pGKTK7-Gal4BD) and Tah1 the prey (pACTII-Gal4AD). Full-length Pih1 and its 253–344 C domain showed similar Y2H interactions with Tah1.

The NMR Structure of Tah1 Bound to the Hsp90 C-Terminal Sequence Reveals How the Short Tah1 TPR Domain Mediates the Interaction

With the nine C-terminal amino acids of yeast Hsp90 (ADTEMEEVD) being sufficient to specifically interact with Tah1 (Millson et al., 2008), we titrated ¹⁵N-labeled Tah1 with this peptide by increasing its concentration up to a 2:1 peptide:protein molar stoichiometry (Figure 4A). The ¹H-¹⁵N HSQC spectra indicate that complex formation is achieved at a 1:1 protein:peptide stoichiometric ratio (data not shown). Tah1 residues showing the largest chemical shift changes upon complex formation belong to residues of the carboxylate clamp (Asn12, Asn43, and Arg83) and residues Tyr27 and Lys50 (Figure S1B). No residues in the C-terminal region showed a significant change in chemical shift consistent with the fact that this unstructured region does not participate in the interaction. We then determined the structure of the complex using a ¹⁵N-¹³C-labeled Tah1 protein bound to an unlabeled Hsp90 peptide. Resonance assignments for the bound peptide were obtained by double-filtered TOCSY and NOESY spectra. The structure was determined using a total of 2,771 NOE-derived distance restraints including 55 intermolecular distance restraints derived from filtered-edited two-dimensional (2D) and three-dimensional (3D) NOESY (Figure 4; Table 1). Tah1 adopts the same fold and organization in the complex as in its free form (Figure S1A) with a backbone rmsd of 0.94 Å (for residues 4–70), indicating that no marked conformational change occurs upon peptide binding. Only helix C undergoes a slight shift toward helix A, which is due to the establishment of a new hydrophobic interaction between residues Leu86 and

Ile49, in addition to the preexisting Ile76–Val39 interaction in the free form (Figure S1A). The C-terminal amino acids remain unfolded in the bound state. This was confirmed by the low relative intensity of ¹H-¹⁵N heteronuclear NOEs of Tah1 in the bound state (Figure S2A).

The first three N-terminal residues of the Hsp90 (A⁷⁰¹D⁷⁰²T⁷⁰³) peptide adopt a rather flexible conformation, in contrast to the six other ones (E⁷⁰⁴MEEEV⁷⁰⁹; Figure 4B). As observed in the CHIP:Hsp90 complex (Zhang et al., 2005), the main chain of the M⁷⁰⁵E⁷⁰⁶E⁷⁰⁷ triplet adopts a turn stabilized by intermolecular H-bonds formed between the two main chain carbonyl groups of M⁷⁰⁵ and E⁷⁰⁷ and the side chain of Tah1 Arg83, which brings the side chain of M⁷⁰⁵ close to the Tah1 helix C (Figure 5A). The backbone atoms of E⁷⁰⁴M⁷⁰⁵E⁷⁰⁶ adopt a 3₁₀ helix structure, enabling the N-terminal extremity of the peptide to exit the protein channel (Figures 4D and 4E). This peculiar structure of the E⁷⁰⁴MEEEV⁷⁰⁷ peptide bound to Tah1, which is stabilized by formation of a H-bond between the main chain of E⁷⁰⁴ and V⁷⁰⁷, is required for its accommodation into the groove of the Tah1 TPR domain (Figures 4C, 4D, and 5).

The highly asymmetric charge distribution between the peptide and Tah1 (Figure S4) results in the establishment of several salt bridges between the positive channel of Tah1 and the negative peptide. These interactions are reinforced by formation of several intermolecular H-bonds and hydrophobic interactions (Figures 5A and S3), explaining the *in vivo* stability of the Tah1:Hsp90 and Tah1(1–92):Hsp90 interactions (Figure 2A). Each of the residues in the EMEEVD sequence participates in the Tah1:TPR recognition. The C-terminal amino acid D⁷⁰⁹ plays a key role in formation of the complex: (1) its lateral chain interacts with three residues of the Tah1 TPR motifs, H-bonds are formed with Asn12 and Asn43 side chains, and one salt bridge

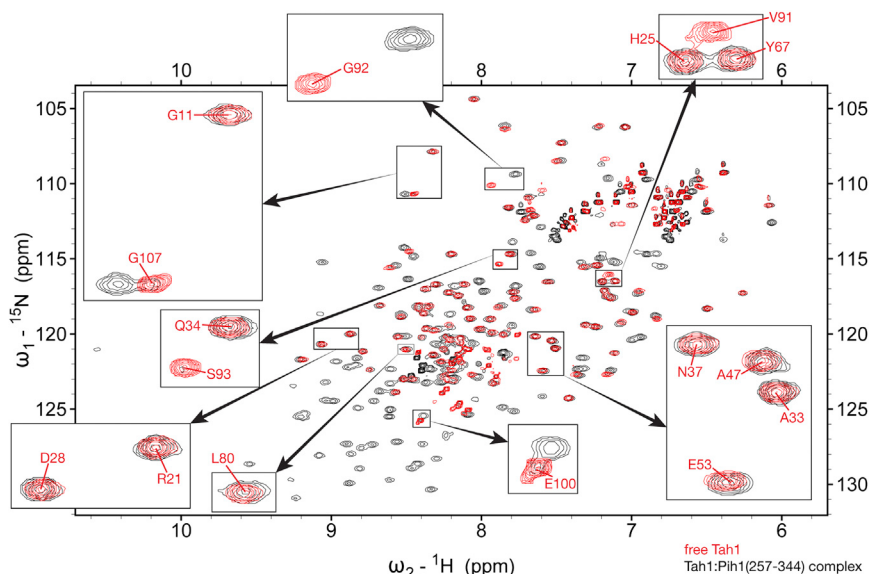


Figure 3. In Vitro Mapping of the Tah1:Pih1(257-344) Interaction by Chemical Shift Perturbation Data

Overlay of the ¹⁵N-¹H HSQC spectra of free Tah1 protein (red) and the Tah1:Pih1(257-344) complex (black). Insets show correlations in free and bound Tah1 of H-N amino acid distributed along Tah1. Assignment corresponds to the free form of Tah1. Some peaks are clearly in intermediate exchange (V91, S93) while other seem to be in slow exchange (G107 and E100). The Tah1 C-terminal region interacts with Pih1(257-344).

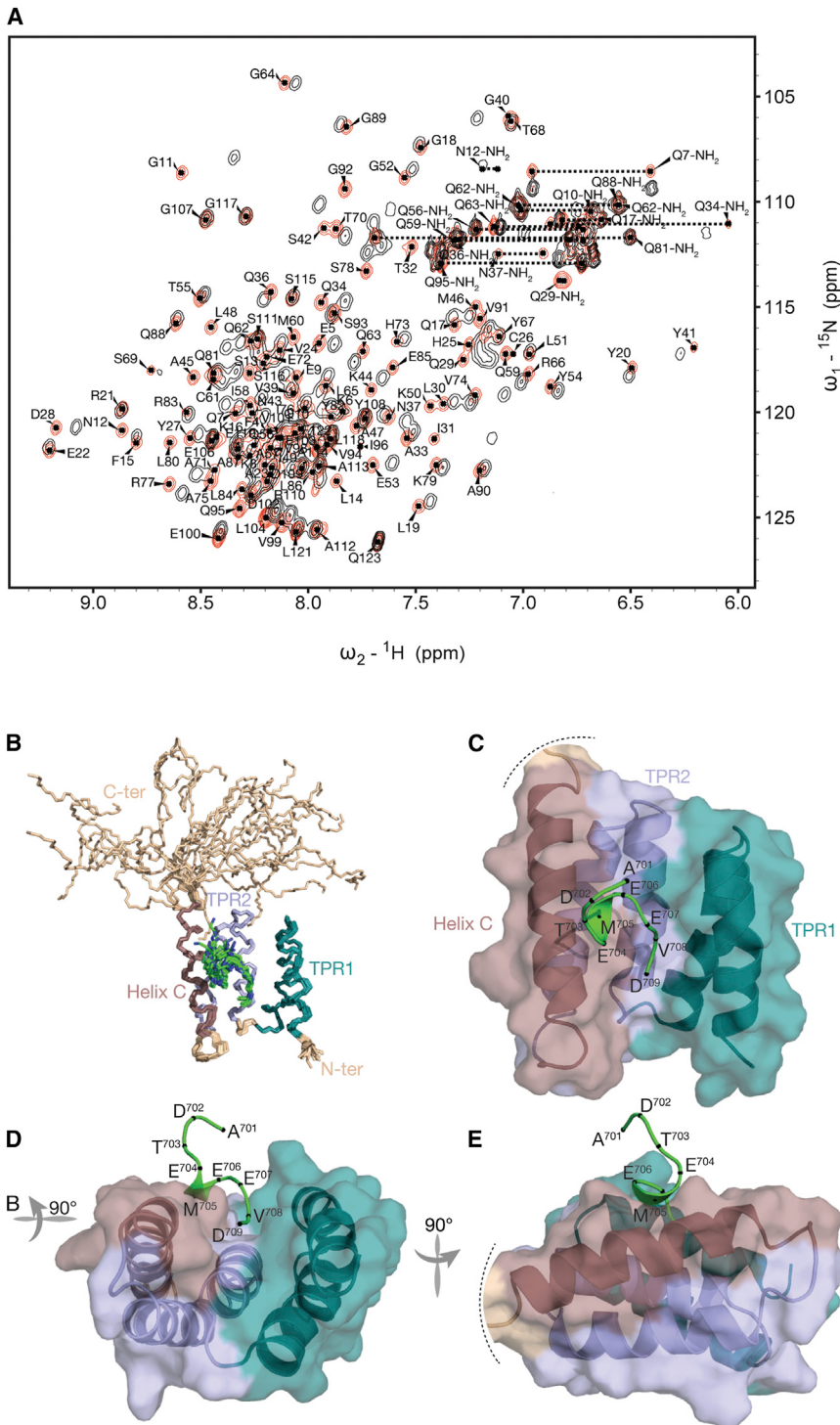
with Lys8 (Figures 5A and S3); (2) its main carboxylate group forms two salt bridges with Lys79 and Arg83 located in helix C; and (3) its main chain amide forms an H-bond with the Asn43 carbonyl side chain (Figures 5A and S3). The V⁷⁰⁸ side chain is located in a hydrophobic pocket formed by Lys8, Lys16, and Phe15 side chains. Its main chain carbonyl group is hydrogen-bonded with the Lys79 side chain (Figures 5 and S3). The carboxylates of residues E⁷⁰⁶ and E⁷⁰⁷ establish salt bridges with the amino groups of Lys50 and Lys16, respectively. The divalent sulfur group of M⁷⁰⁵ specifically interacts with the π electron of Tyr82 aromatic cycle (Meyer et al., 2003a), and its methyl group is positioned between the methylene of Tyr82 and the aliphatic side chain of Lys79 (Figure 5). Finally, the carboxylate and main chain carbonyl of E⁷⁰⁴ both interact with the amino side chain of Lys79. No interaction was observed between A⁷⁰¹, D⁷⁰², and T⁷⁰³ of Hsp90 and Tah1. Our structure shows that both the two canonical TPR motifs of Tah1 and helix C interact with the Hsp90 EMEEVD segment. The helices 1A and 2A of the TPR together contribute to the formation of one hydrophobic interaction, four salt bridges, and three H-bonds. Helix C contributes to the formation of nine interactions with the EMEEVD peptide: one hydrophobic interaction, three salt bridges, and five H-bonds, underlying the crucial role of this additional helix C for the interaction with Hsp90.

Residues in Tah1 Helix C Are Essential for the Interaction with Hsp90

To confirm the functional importance of helix C in the Tah1:Hsp90 interaction in cellulo, we individually substituted the Tah1 Lys79, Tyr82, and Arg83 residues and the Hsp90 E⁷⁰⁶, E⁷⁰⁷, V⁷⁰⁸, D⁷⁰⁹ residues with alanine and tested the effects of these mutations on the Hsp90:Tah1 interaction with Y2H assays (Figure 6). As a control, Arg77, Glu85 in the Tah1 helix C, and D⁷⁰², T⁷⁰³ in Hsp90, which are not involved in the protein-peptide interaction, were also substituted. We controlled the expression of the mutated Tah1 and Hsp90 proteins by testing their interactions with Pih1 using Y2H assays. In perfect agree-

ment with our structure, Lys79Ala, Tyr82-Ala, and Arg83Ala substitutions in Tah1 helix C abolished the interaction with Hsp90, but did not affect the Tah1:Pih1 interaction (Figure 6A). In addition, in agreement with our structure, substitutions of Arg77 or Glu85 had no effect on any of the interactions. Concerning Hsp90, the D⁷⁰⁹A substitution completely abolished the interaction with Tah1, confirming the crucial role of the C-terminal D⁷⁰⁹ (Figure 6B). The interaction was weakened by the E⁷⁰⁶A and V⁷⁰⁸A substitutions, but the effect was less pronounced than for the other mutants. The E⁷⁰⁷A mutation had a more limited negative effect. However, E⁷⁰⁷ implication was evidenced by a significant decrease of the 3-AT resistance. As expected, mutations of amino acids D⁷⁰² and T⁷⁰³ had no marked effect. These results confirmed the functional importance of the Tah1 helix C for in vivo interaction of Tah1 with Hsp90.

The effects of several amino substitutions in Tah1 on affinity of Tah1-Hsp90 peptide interaction had already been studied in vitro by isothermal titration calorimetry (ITC) measurements (Jiménez et al., 2012; Millson et al., 2008). However, because our 3D structure revealed yet unidentified amino acid interactions involving Tyr82 of helix C, to get a quantitative evaluation of their importance, this residue was mutated into an alanine and the effect on the affinity of the Tah1-ADTEMEEVD interaction was tested with ITC. As a control, Lys79, which was already known to play an important role in the interaction, was also mutated into alanine (Jiménez et al., 2012). The dissociation constant (K_D) for the ADTEMEEVD:Tah1 complex established at 20°C in the NMR buffer was $5.41 \pm 0.33 \mu\text{M}$ with a molar stoichiometry of 1:1 (Table 2; Figure S5) similar to that obtained with NMR titration experiments (Figure 4A). The lower K_D value (factor of about 10) observed for WT Tah1 as compared to those in the studies of Jimenez and Millson and their colleagues (Jiménez et al., 2012; Millson et al., 2008) is due to the use of different experimental conditions (Tris buffer with 5 mM NaCl instead of phosphate buffer with 150 mM NaCl, experiments performed at 4°C instead of 20°C). Not surprisingly, as found by Jimenez and colleagues, the Lys79A mutation in Tah1 abolished the interaction with the Hsp90 peptide and the same result was observed for the Tyr82A mutation (Table 2; Figure S5). These in vitro data are in line with our Y2H results (Figure 6), confirming the direct and strong implication of helix C for binding of Tah1 to the Hsp90 C-terminal peptide.



DISCUSSION

Here, we report the high-resolution solution structures of protein Tah1 in free form and in complex with the C-terminal Hsp90 peptide (ADTEMEEVD). Recently, a solution structure of the same protein bound to the MEEVD motif of Hsp90 was proposed (**Ji**

Tah1 TPR domain in our structure are superimposable to corresponding helices in the CHIP and Hop TPR2A bound TPR domains (overall average rmsd of 1 Å with the CHIP TPR and Hop TPR2A domains; Figure 7). Furthermore, the polarities of the bound peptides are also identical. In these comparisons, the Tah1 helix C takes the place of helix 3A in the third TPR motifs

Figure 4. NMR Structure of the Tah1:Hsp90 Peptide Complex

(A) Chemical shift mapping of the Tah1:Hsp90 peptide interaction by titration. $^{15}\text{N}-^1\text{H}$ HSQC spectral overlays of free (black) and bound (red) Tah1 (1:1 protein:peptide molar ratio).

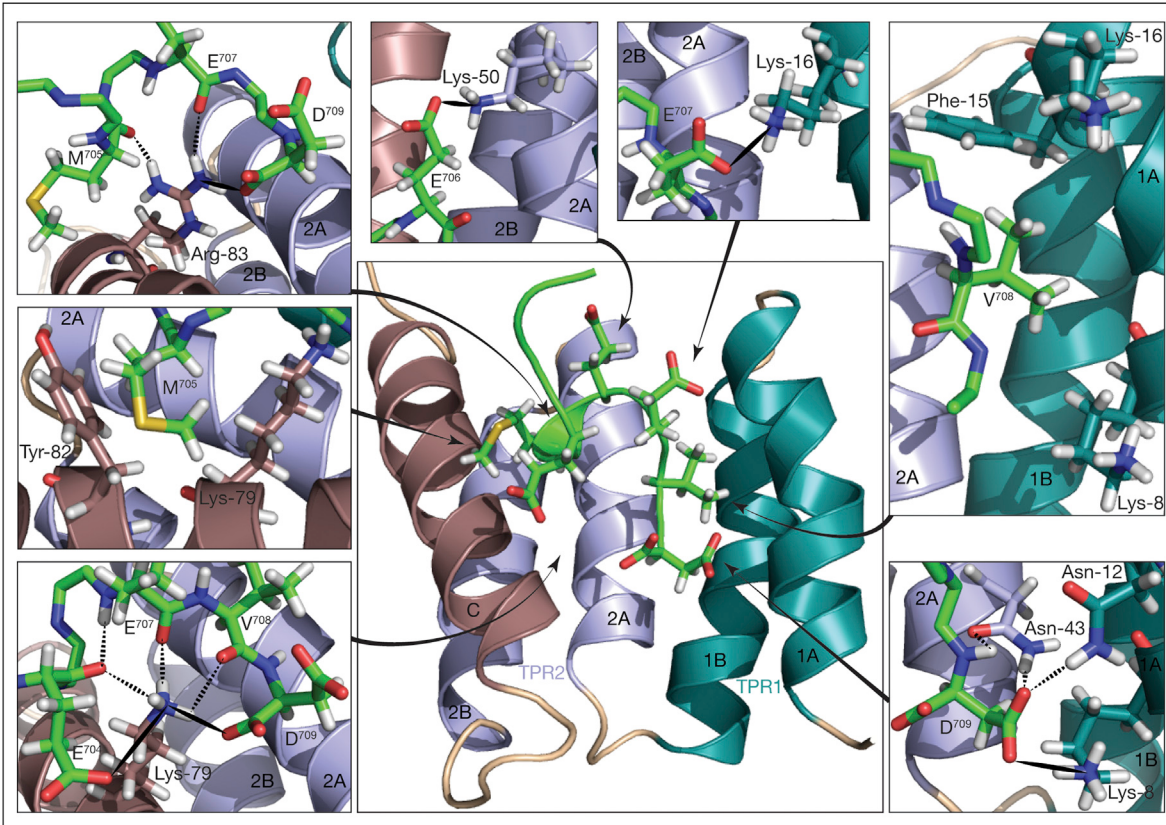
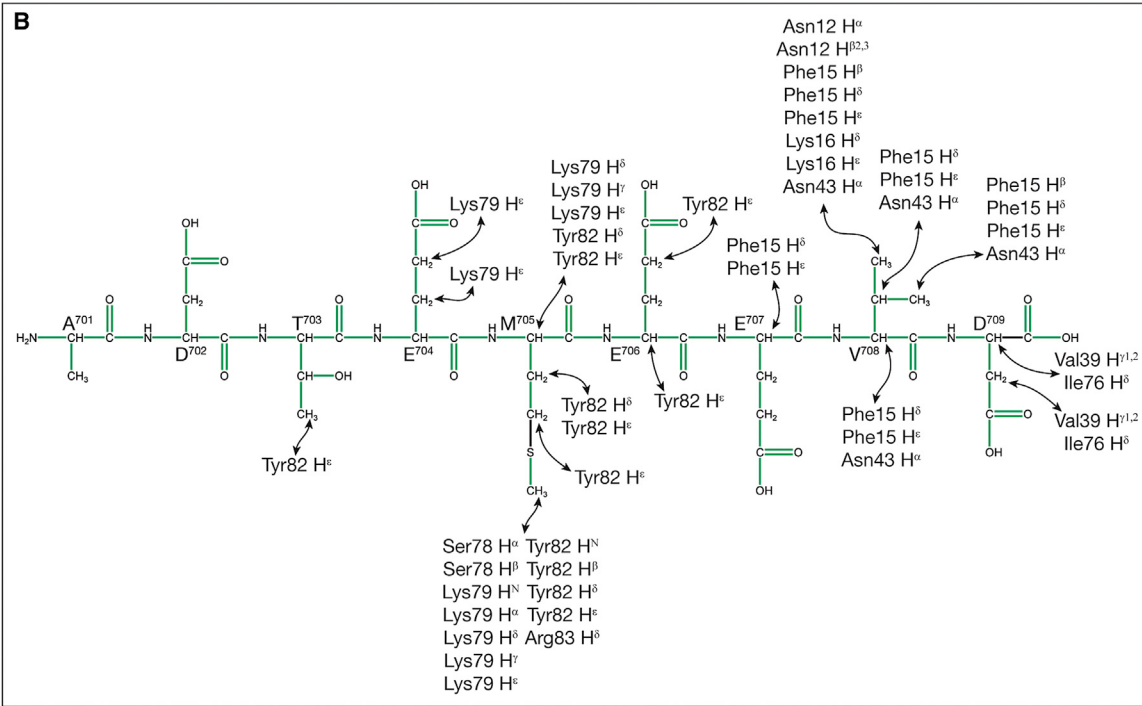
(B) NMR structures of Tah1 bound to the C-terminal peptide of Hsp90. Among the 50 final calculated structures, 20 were selected for their lowest total energy (same color code as in Figure 1).

(C-E) Front (C), bottom (D), and side (E) views of the Tah1:Hsp90 lowest energy conformer. PyMOL transparent surface of bound Tah1 with ribbon representation of the protein chain; the unfolded C-terminal domain is not displayed. The ribbon representation of the Hsp90 peptide backbone is in green and the amino acids are labeled (black sphere at each $\text{C}\alpha$).

See also Figures S1, S2, and S4.

ménez et al., 2012). However, due to the intermolecular NOE information, the authors had to combine various approaches, including NMR titration assays, site-directed mutagenesis, and 3D structure modeling, to get a 3D model of the MEEVD:Tah1 complex. Although both studies identified a short TPR domain that is formed by two TPR motifs and is capped by an helix denoted C, and a flexible C-terminal domain in Tah1, our 3D structure of the bound Tah1 differs from their structure (rmsd for bound Tah1 of 2.5Å; Figure 7A). Moreover, two major differences concern the orientation and conformation of the Hsp90 peptide in the TPR groove. Indeed, the conformation of our bound peptide is not linear, and its N and C-terminal ends are inverted (Figure 7A). Importantly, our positioning of the peptide in the Tah1 groove was determined with 55 intermolecular NOEs (Figure 5B) at a stoichiometric ratio, while Jimenez and colleagues only observed five intermolecular NOEs at a very high 1:10 protein-to-peptide molar ratio. Therefore, we are confident that the orientation and conformation of the peptide in our complex are accurate.

Furthermore, in contrast to the Tah1:-MEEVD model proposed by Jiménez and colleagues and in agreement with data in the literature, helices of the bound

A**B****Figure 5. The Six C-Terminal Amino Acids of Hsp90 Interact with the Tah1 TPR Domain**

(A) Topology of the Tah1:Hsp90 interaction. A complete view of the interaction with ribbon representation of Tah1 and stick representation of the peptide is shown at the center. Magnified views of the various zones of interactions are shown in the insets. For clarity, some of them are rotated relative to the central panel.

(legend continued on next page)

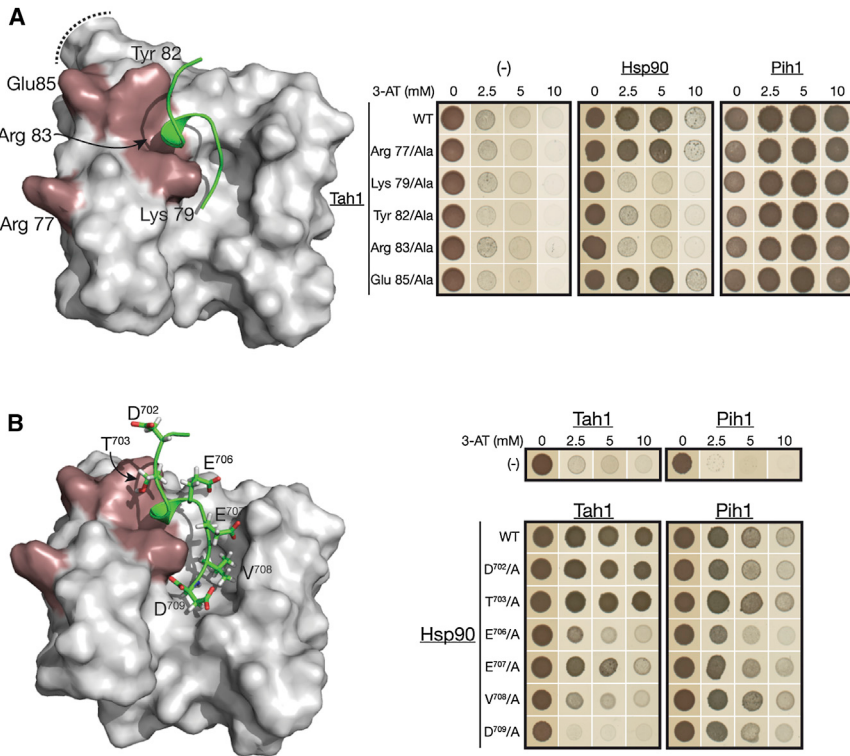


Figure 6. Dissecting the Tah1 Helix C and Hsp90 Amino Acids Critical for Tah1:Hsp90 Interaction In Vivo

(A) Tah1 Lys79, Tyr82, and Arg83 play a critical role for Tah1-Hsp90 interaction in vivo. Y2H assays were performed as in Figure 2, using 3-amino-1,2,4-triazol (3AT) as a competitive inhibitor of the *HIS3* gene product. WT Tah1 and its variants were the bait (pGKKT7-Gal4BD) and Hsp90 or Pih1 the prey (pACTII-Gal4AD). The Hsp90 interaction with Tah1 was abrogated by Lys79Ala, Tyr82Ala, or Arg83Ala substitutions, while Arg77Ala and Glu85Ala had no negative effects. Positive Y2H interactions between Tah1 variants and Pih1 (right picture) confirmed the correct expression of Tah1 variants. On the left, the positions of the five mutated amino acids are shown on molecular surface of the Tah1:Hsp90 structure.

(B) Implication of Hsp90 D⁷⁰⁹, V⁷⁰⁸, and E⁷⁰⁶ for the Tah1:Hsp90 in vivo interaction as evidenced by Y2H assays in the right panel. Hsp90 and its variants were used as the prey (pACT2-Gal4AD) and Tah1 or Pih1 as the bait (pGKKT7-Gal4BD). In the left image, the positions of the mutated Hsp90 amino acids are shown on the molecular surface of the Tah1:Hsp90 structure.

of CHIP and Hop, and the Tah1 carboxylate clamp residues (Lys8, Asn12, Asn43, Lys79, and Arg83) superimpose onto the equivalent carboxylate clamp residues of the bound CHIP and Hop TPR domains (Figures 1C and 8). Accordingly, when Jiménez and colleagues individually substituted these five Tah1 residues into alanine, the in vitro binding affinity of the MEEVD peptide for Tah1 mutants was either reduced (Lys 8 and Asn12) or abolished (Asn43, Lys79, and Arg83) as estimated by ITC experiments (Jiménez et al., 2012). Our 3D structure fully explains these in vitro data and our Y2H data confirm the crucial role of the helix C residues Lys79 and Arg83 for interaction of Tah1 with full-length Hsp90 in vivo.

In our 3D structure of bound Tah1, each of the six C-terminal amino acids (E⁷⁰⁴MEEVD⁷⁰⁹) of the Hsp90 tail are involved in the interaction with Tah1. As observed in complexes formed with the HOP, CHIP, and Tom71 proteins, the E⁷⁰⁷V⁷⁰⁹ segment of Hsp90 adopts an extended conformation (Li et al., 2009; Scheufler et al., 2000; Zhang et al., 2005) and most of the interactions established between the E⁷⁰⁶EVD⁷⁰⁹ motif and Tah1 are similar to those found for the human PP5 (Russell et al., 1999) and Hop (Brinker et al., 2002) proteins. Therefore, the interactions established with this E⁷⁰⁶EVD⁷⁰⁹ motif are not expected to play an important role for the specific recognition of Tah1 by Hsp90. The specificity of the Tah1-Hsp90 interaction mainly depends upon interactions established between the Tah1

helix C and the Hsp90 amino acids located upstream from the E⁷⁰⁶EVD⁷⁰⁹ motif. It is well known that the Hsp90 M⁷⁰⁵ residue, which is replaced by an isoleucine in Hsp70, is one key element in the specific recognition of TPRs by Hsp90 (Brinker et al., 2002; Scheufler et al., 2000). Furthermore, interactions between TPRs and Hsp90 amino acids located upstream of EEVD were found to differ from one TPR domain to the other (Figure 8; Scheufler et al., 2000; Zhang et al., 2005). The specific feature of the Hsp90:Tah1 recognition is due to the peculiar conformation of the peptide backbone at the level of M⁷⁰⁵. The main chain of the E⁷⁰⁴ME⁷⁰⁶ residues forms a 3₁₀ helix (followed by a turn), which projects M⁷⁰⁵ in close contact with the Tah1 helix C. This peculiar conformation results from formation of an S-CH3/π interaction between sides chains of M⁷⁰⁵ and Tah1 Tyr82. The need for this S-CH3/π interaction explains the complete loss of binding of the Hsp90 peptide to Tah1 carrying a Tyr82Ala mutation that we observed in vitro with ITC analysis and our negative Y2H assay when using this variant. The requirement of the S-CH3/π interaction in the Tah1:Hsp90 complex also explains why a M⁷⁰⁵V mutation in yeast Hsp90 decreased the in vitro binding of Tah1 by a factor of 20 (Millson et al., 2008). In the MEEVD:Hop-TPR2A complex, the orientation of one end of the peptide chain is different as compared to that in the Tah1-Hsp90 complex because M⁷²⁸ (the counterpart of yeast Hsp90 M⁷⁰⁵) is closer to helix 1A (Figures 7B and 8B) and forms

Hydrogen bonds and salt bridges are symbolized by dotted and full lines, respectively. The left and right insets show the numerous interactions established between helices 2A and C, and 2A and 1A, respectively.

(B) Details of the 55 intermolecular NOEs of the Tah1:Hsp90 peptide interface. The sequence of the Hsp90 C-terminal peptide (ADTMEEVD) was developed and the amino acids labeled. The type, name, and residue position in the Tah1 sequence of each proton giving NOE cross-peaks with the peptide are shown with arrows.

See also Figures S3 and S4.

Table 2. Thermodynamic Parameters Established for the Interaction of the ADTEMEEVD Peptide with Protein Tah1 and Its Mutants

Protein	K_D (μM)	ΔG (kcal/mol)	ΔH (kcal/mol)	ΔS (cal/mol/K)	n
Tah1 WT (SD)	5.41 (0.33)	-6.84 (0.06)	-5.9 (0.06)	3.2	0.98 (0.007)
Tah1 (K79A)	no binding	no binding	no binding	no binding	no binding
Tah1 (Y82A)	no binding	no binding	no binding	no binding	no binding

See also Figure S5.

a hydrophobic interaction with the Hop Tyr236 residue (Figures 8A and 8B). In the CHIP:Hsp90 complex, because an S-CH3/ π interaction involving human Hsp90 α M⁷²⁸ equivalent to yeast Hsp90 M⁷⁰⁵ and CHIP Phe99 is formed, the peptide chain orientation is comparable to that in the Tah1-Hsp90 complex. These comparisons illustrate how the type of interaction formed by M⁷⁰⁵ participate to the specificity and orientation of the chaperone tail in the TPR:Hsp90/70 interactions.

Because of the E⁷⁰⁴MEEVD⁷⁰⁹ backbone orientation, the main and side chains of Lys79 in Tah1 interact with E⁷⁰⁴. The absence of detection of interactions with E⁷⁰⁴ in structures previously published might simply be explained by the very limited number of structural analyses performed with peptides longer than five residues, namely, (M/I)EEVD (Cliff et al., 2006; Jiménez et al., 2012; Li et al., 2009; Scheufler et al., 2000; Zhang et al., 2005). However, the choice of using short peptides was justified by the initial observation of the low influence of residues located upstream of residue M⁷⁰⁵ on TPR binding (Scheufler et al., 2000). In agreement with our structural data, previous results showed that the binding affinity of Tah1 for the Hsp90 MEEVD peptide increases by a factor of 30 upon addition of the T⁷⁰³E⁷⁰⁴ amino acids (Millson et al., 2008).

Whereas the Tah1 TPR domain adopts a highly folded structure both in free and bound Tah1, the C-terminal part of Tah1 remains unfolded in the presence or the absence of the Hsp90 peptide. Based on in vitro binding assays, the C-terminal region of Tah1 was previously proposed to interact with Pih1 (Eckert et al., 2010; Zhao et al., 2005). However, the segment required was not precisely delineated. We found that the unfolded C-terminal segment (93–111) of Tah1 is sufficient to associate with the Pih1 253–344 segment in Y2H and only residues in region 91–111 of the full-length Tah1 shift upon addition of Pih1 257–344 in NMR assays. In contrast to previous data of Paci and colleagues (Paci et al., 2012), the Pih1 A²⁵¹PAPAP²⁵⁶ amino acid cluster is not essential for interaction with Tah1. Accordingly, this cluster is not conserved in the homologous human PIH1D1 protein, which interacts with RPAP3, the human homolog of Tah1 (Boulon et al., 2008). Our NMR spectrum of the Tah1:Pih1(257–344) complex strongly suggests that the C-terminal part of Tah1 folds upon interaction with Pih1. Altogether, our data strongly support the idea that the unfolded part of Tah1 is sufficient to establish a stable interaction with Pih1.

The specific biologic activities carried by cochaperones are associated with specific domains in addition to the TPR domain: e.g., a phosphatase domain in PP5, a peptidylprolyl isomerase domain in FKBP52, and an ubiquitin ligase domain in CHIP. Tah1 lacks such specific activity. The short Tah1 sequence, which is not included in the TPR domain (position 91–111), serves as a Pih1 recruiting site. The capacity to negatively modulate the Hsp90 ATPase activity is carried out by Pih1 (Eckert

et al., 2010), while Tah1 alone exhibits only a very weak stimulation activity on Hsp90 (Millson et al., 2008). Tah1 stabilizes Pih1 in vitro and mediates its association with Hsp90. Therefore, the Pih1:Tah1 heterodimer can be considered as the functional entity able to specifically recognize Hsp90 and to negatively modulate its activity. However, the mechanism of action of the Pih1:Tah1 complex in regulation of the Hsp90 cycle remains to be elucidated. Our data are a step in the determination of the 3D structure of the Tah1:Pih1 complex that will be important to decipher how the R2TP-Hsp90 complex is implicated in the snoRNP and RNA polymerase assembly.

EXPERIMENTAL PROCEDURES

Biologic Material Used in This Study

The *S. cerevisiae* strains Y190 and Y187 and plasmids pACTII::PIH1, pACTII::HSP82 (wild-type [WT] and mutants), pACTII::TAH1, pGBKT7::TAH1 (WT, domains, and mutants), and pGK77::PIH1 (WT and domains) were used for Y2H assays (see Supplemental Experimental Procedures). To express Tah1-His₆, a cDNA encoding full-length Tah1 was cloned into plasmid pKHS in which a cleavage site for the PreScission protease had been inserted (Eckert et al., 2010). Because of the need of compatible plasmids for protein coexpression in *E. coli*, we used plasmids pET15b and pACYC18b-11b for coexpression of His₆-Tah1 and Pih1(254–344) (Diebold et al., 2011). *E. coli* BL21 DE3 pRare2 host cells (Novagen) were used for production of both Tah1-His₆ and the His₆-Tah1:Pih1(257–344) complex. The Hsp90 ADTEMEEVD peptide was purchased from GenCust (Luxembourg).

Production and Purification of the ¹⁵N-¹³C-Labeled Tah1 Recombinant Protein

The recombinant Tah1-His₆ protein was purified as described previously (Eckert et al., 2010). The Ni-Sepharose bound protein was eluted with an imidazole gradient, dialyzed in 20 mM Tris HCl (pH 7.5) and 150 mM NaCl and bound again on Ni-sepharose high-performance beads. Free Tah1 was released by cleavage with the PreScission protease (5–10 U/mg of protein) overnight at 4°C. Residual impurities and the protease were removed with size exclusion chromatography using a Superdex 75 prep grade column (GE Healthcare) equilibrated with the NMR buffer (10 mM Na₂HPO₄/Na₂HPO₄ [pH 7.2] and 150 mM NaCl). The protein was stored in this buffer at -20°C at 1 mM.

Production of Uniformly ¹⁵N-Labeled Tah1:Pih1(257–344) Complex in *E. coli* and Its Purification

We coexpressed His₆-Tah1 and the Pih1(257–344) fragment by cotransformation of *E. coli* BL21 DE3 pRare2 cells (Novagen) pET15b and pACYC18b-11b. Growth was performed in 2 l of N¹⁵-labeled M9 minimal medium at 37°C until reaching absorption at 600 nm (A_{600}) of 0.8. Then, the temperature was switched to 20°C and protein coexpression was induced by the addition of 1 mM isopropyl-β-D-thiogalactopyranoside (Euromedex). Cells were further grown overnight at 20°C, collected, suspended in buffer A (20 mM HEPES-NaOH, pH 7.5; 150 mM NaCl; and 5 mM β-mercaptoethanol), and lysed by sonication. The soluble fraction was mixed with 3 ml of Talon beads (Clontech), incubated for 1 hr at 4°C. After centrifugation and extensive washing with buffer A, the complex was eluted by overnight cleavage at 4°C, using the PreScission protease (5–10 U/mg of protein). The protease and other

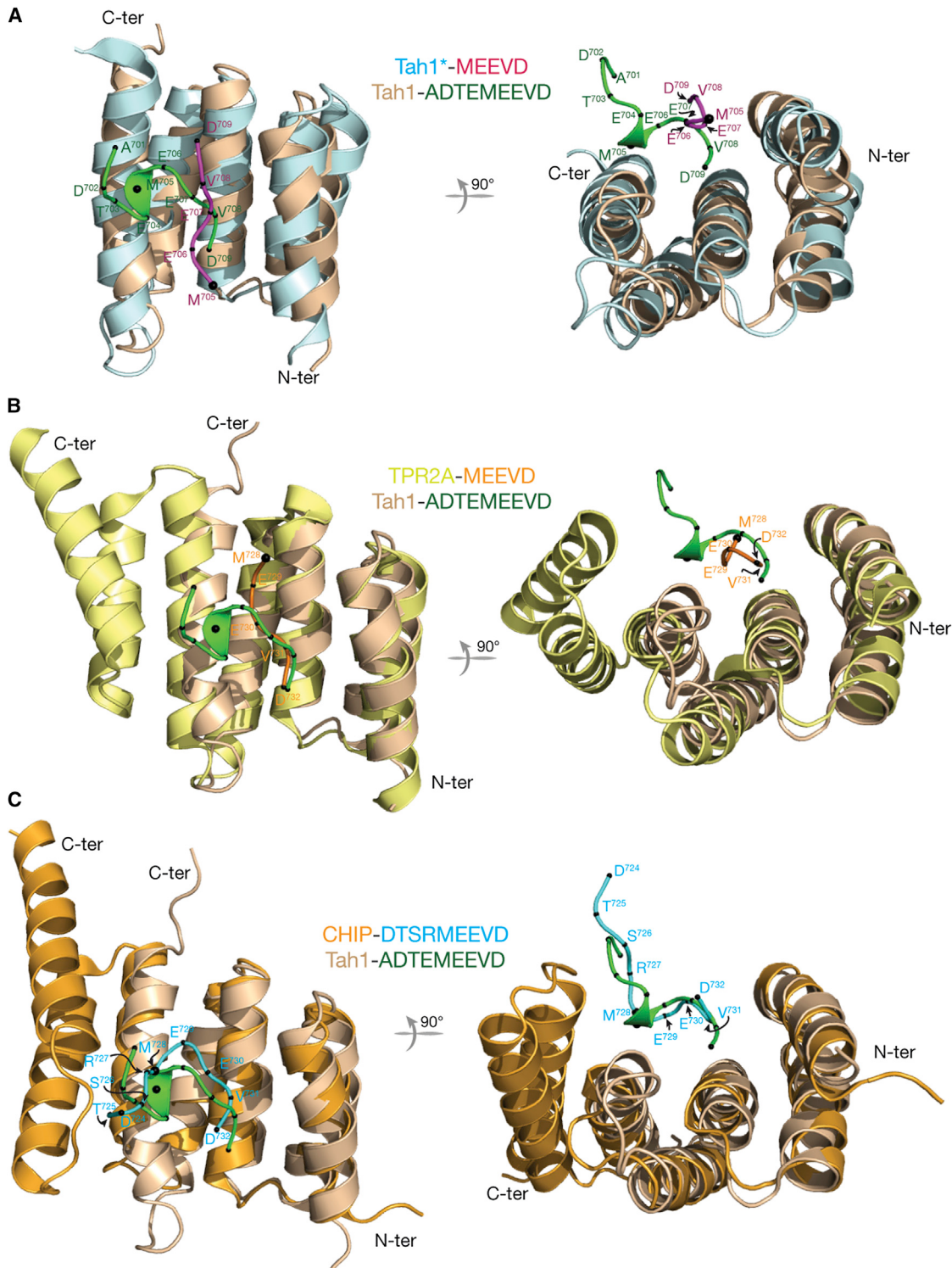
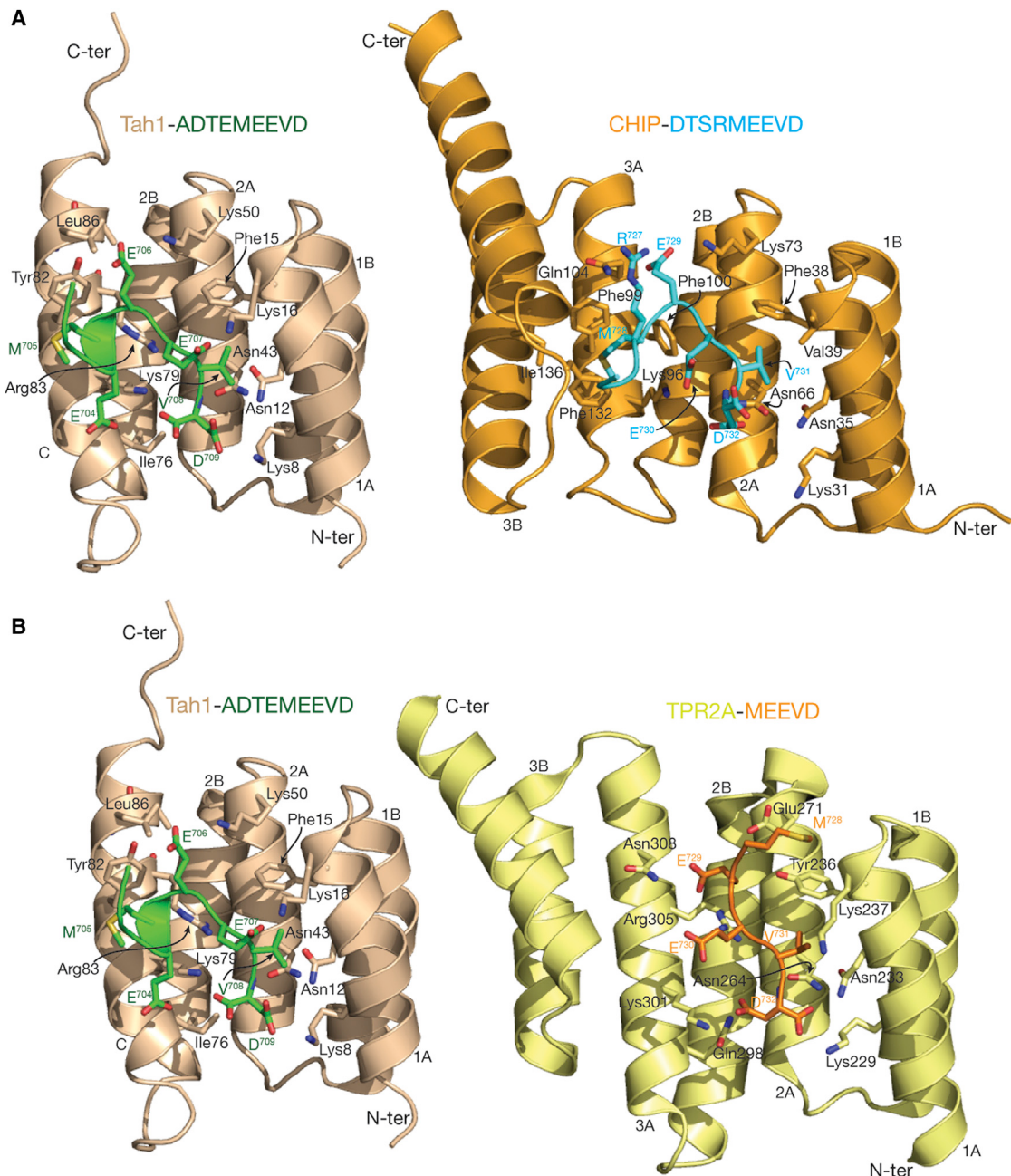


Figure 7. Comparison of the Bound Tah1, Hop TPR2A, and CHIP TPR Domains

Our yeast Tah1:ADTEMEEVD structure is overlaid on the structures of yeast Tah1*:MEEVD (2L6J; Jiménez et al., 2012; A), human Hop TPR2A:MEEVD (1ELR; Scheufler et al., 2000; B), and mouse CHIP: human DTSRMEEVD (2C2L; Zhang et al., 2005; C) complexes. Ribbon representation of the Tah1 TPR in wheat is overlaid on each of the other TPR domains. The C α traces of the Hsp90 peptides are in pink (structure of Jiménez and colleagues), green (our structure), orange (TPR2A complex), and blue (CHIP complex), respectively, and alpha carbons of peptide residues are indicated by full black spheres. All right-side views are rotated by 90°. The structure alignments were performed by PyMOL using the backbone of 4–70 residues. The best superimposition obtained is with bound Hop TPR2A and CHIP TPR structures.

**Figure 8. Detailed Comparison of the Complexes**

Tah1:ADTEMEEVD complex with CHIP:DTSRMEEVD (A) and TPR2A:MEEVD (B). Representation and color codes are the same as those in Figure 7. The side chains of residues in intermolecular interactions are represented as stick forms and are labeled. The side chains of ADT and DTS residues in peptides bound to Tah1 and CHIP, respectively, are not represented for clarity.

impurities were eliminated with Superdex 75 (GE Healthcare) size exclusion chromatography (GE Healthcare) using the NMR buffer. The complex was stored at -20°C , at a 1 mM concentration in the NMR buffer.

NMR Measurements

NMR spectra of free Tah1 were recorded at 288 K on a BRUKER DRX 600 US spectrometer equipped with a triple resonance (^1H , ^{15}N , and ^{13}C) TCI Z 5 mm cryoprobe using a ^{15}N - ^{13}C -labeled Tah1 sample (~ 1 mM). Data were processed by Topspin (Bruker) and analyzed with the Sparky 3.113 software (Goddard and Kneller, 2002). Sequence-specific backbone, side chain, and

aromatic proton assignments were achieved using 2D and 3D classical experiments (see Supplemental Experimental Procedures).

HSQC spectra of the Tah1:Pih1(257–344) complex were recorded on the same spectrometer in the same conditions using the N^{15} -labeled complex (~ 1 mM).

NMR measurements for the assignment of the Tah1: peptide complex were performed in the same conditions as above using Bruker AVIII-500 MHz, AVIII-700 MHz, and Avance-900 MHz spectrometers. The samples were prepared at an ~ 1 mM concentration using ^{15}N - ^{13}C -labeled Tah1 and unlabeled yeast Hsp90 peptide at a 1:1 molar ratio. We assigned the bound Tah1 backbone,

side chains, and aromatic protons using 2D and 3D experiments described in the [Supplemental Experimental Procedures](#). We assigned protons of the bound Hsp90 peptide in the Tah1:peptide complex by using 2D F1-filtered, F2-filtered TOCSY, and 2D F1-filtered, F2-filtered NOESY experiments in H₂O or 100% D₂O.

Intermolecular NOEs were obtained from 3D ¹⁵N F1-filtered, F2-edited NOESY-HSQC, 3D ¹³C F1-filtered, F3-edited NOESY-HSQC experiments in H₂O or 100% D₂O, and 2D ¹³C F1-filtered, F2-edited NOESY performed on the ¹⁵N-¹³C Tah1:peptide complex.

Structure Calculation and Refinement

The automated peak picking, NOE assignment, and structure calculation of free and bound Tah1 were performed using the Atnos/Candid software ([Herrmann et al., 2002a, 2002b](#)). We used (1) 3D ¹⁵N and ¹³C NOESY-HSQC, and 2D homonuclear NOE spectra recorded in D₂O for structure analysis of free Tah1; (2) 3D ¹⁵N and ¹³C NOESY-HSQC experiments for structure determination of the bound protein, and (3) 2D ¹³C F1-filtered F2-filtered NOESY in H₂O or 100% D₂O for structure analysis of the bound peptide. Seven iterations were performed, and 250 independent structures were calculated at each iteration step.

We used the CYANA software to calculate the structures of the Tah1:Hsp90 peptide complex, which was based on a list of automatically assigned intramolecular NOE distance constraints that we established for the bound Tah1 and bound peptide using the Atnos/Candid software and manually assigned intermolecular distance constraints for the complex ([Güntert, 2004](#)).

The 50 structures with the lowest energy were refined using the AMBER 7.0 software with simulated annealing protocol ([Case et al., 2005](#)). We analyzed the 20 best final structures based on energy, NOE violations, and structural quality using PROCHECK software ([Laskowski et al., 1996](#)).

Isothermal Titration Calorimetry

Binding properties of the synthetic ADTEMEEVD peptide to purified WT and variant Tah1 proteins were studied at 20°C in NMR buffer on a VP-ITC microcalorimeter (MicroCal). Protein concentrations were determined from A₂₈₀ measurements performed on a nanodrop spectrophotometer 2000c. The synthetic peptide containing an acetyl moiety at the N terminus and a free C-terminal carboxylate group was accurately weighed on an analytical balance M-120 (Denver Instrument) and dissolved in NMR buffer. Samples were filtered and degassed. The heat of dilution was determined in a separate experiment by diluting the peptide into NMR buffer. In each experiment, we performed 50 injections of 5 µl of a 1.1 mM peptide solution into the 1.4288 ml chamber containing WT or mutant Tah1 at a 90 µM concentration. The syringe speed was set at 300 rpm and a 200 s delay time was maintained between each injection. After subtraction of dilution heats, calorimetric data were analyzed using a nonlinear least square curve-fitting algorithm provided by the manufacturing (Origin version 7) with four parameters: stoichiometry (n), association constant (K_a), variation in enthalpy (ΔH), and in entropy (ΔS). Gibbs free energy (ΔG) was calculated by using the Gibbs free energy equation (ΔH-TΔS).

Yeast Two-Hybrid Assays

Recombinant plasmids obtained after cloning the various protein coding sequences into plasmids pACTII (*LEU2*) and pGBTKT7 (*TRP1*) were used to transform haploid cells (strains Y190 and Y187, respectively). After mating, the diploid cells were selected on media suitable for double selection (Leu⁻ and Trp⁻), and interaction tests were performed after plating the cells on media suitable for triple selection (Leu⁻, Trp⁻, and His⁻). Various concentrations of 3-amino-1,2,4-triazol were used to evaluate the strength of the interactions. Growth was assessed after 3 days of incubation at 30°C.

ACCESSION NUMBERS

The Protein Data Bank accession numbers for the coordinates of the free and bound Tah1 structures are 2LSU and 2LSV, respectively. The Biological Magnetic Resonance Bank accession numbers for the resonance assignments of free and bound Tah1 are 18445 and 18447, respectively.

SUPPLEMENTAL INFORMATION

Supplemental Information includes Supplemental Experimental Procedures and five figures and can be found with this article online at <http://dx.doi.org/10.1016/j.str.2013.07.024>.

ACKNOWLEDGMENTS

This work was supported by the French Agence Nationale pour la Recherche (ANR 06-BLAN-0208-02, ANR 11 BSV8 015 03, and ANR-05-JCJC No. 015101), the French Centre National de la Recherche Scientifique, Lorraine University, the Plan Etat Région Lorraine (Bioengineering program), the European EURASNET network (LSHG-CT-2005-518238), the French Ligue Nationale contre le cancer Grand-Est (No.30025555), and the French Association pour la Recherche contre le Cancer (SFI20101201793). R.B. and B.R. were fellows from the French Ministère de l'Enseignement Supérieur et de la Recherche. Use of the NMR and ITC facilities of the Service Commun de Biophysicochimie des Interactions Moléculaires were deeply appreciated. We gratefully acknowledge Drs. Judith Osz and Catherine Birck (Structural Biology and Genomics Platform, IGBMC, Illkirch, France) for their advice during ITC experiments. Stays of R.B. in the F.H.-T.A Lab were supported by the exchange program of the EURASNET network. Research in the F.H.-T.A. lab was supported by the NCCR-SNF structural biology and the ETH Zurich.

Received: July 2, 2012

Revised: July 3, 2013

Accepted: July 10, 2013

Published: September 5, 2013

REFERENCES

- Ali, M.M., Roe, S.M., Vaughan, C.K., Meyer, P., Panaretou, B., Piper, P.W., Prodromou, C., and Pearl, L.H. (2006). Crystal structure of an Hsp90-nucleotide-p23/Sba1 closed chaperone complex. *Nature* 440, 1013–1017.
- Boulon, S., Marmier-Gourrier, N., Pradet-Balade, B., Wurth, L., Verheggen, C., Jády, B.E., Rothé, B., Pescia, C., Robert, M.C., Kiss, T., et al. (2008). The Hsp90 chaperone controls the biogenesis of L7Ae RNPs through conserved machinery. *J. Cell Biol.* 180, 579–595.
- Boulon, S., Pradet-Balade, B., Verheggen, C., Molle, D., Boireau, S., Georgieva, M., Azzag, K., Robert, M.C., Ahmad, Y., Neel, H., et al. (2010). HSP90 and its R2TP/Prefoldin-like cochaperone are involved in the cytoplasmic assembly of RNA polymerase II. *Mol. Cell* 39, 912–924.
- Brinker, A., Scheufler, C., Von Der Mulbe, F., Fleckenstein, B., Herrmann, C., Jung, G., Moarefi, I., and Hartl, F.U. (2002). Ligand discrimination by TPR domains. Relevance and selectivity of EEVD-recognition in Hsp70 x Hop x Hsp90 complexes. *J. Biol. Chem.* 277, 19265–19275.
- Case, D.A., Cheatham, T.E., 3rd, Darden, T., Gohlke, H., Luo, R., Merz, K.M., Jr., Onufriev, A., Simmerling, C., Wang, B., and Woods, R.J. (2005). The Amber biomolecular simulation programs. *J. Comput. Chem.* 26, 1668–1688.
- Cliff, M.J., Harris, R., Barford, D., Ladbury, J.E., and Williams, M.A. (2006). Conformational diversity in the TPR domain-mediated interaction of protein phosphatase 5 with Hsp90. *Structure* 14, 415–426.
- Connell, P., Ballinger, C.A., Jiang, J., Wu, Y., Thompson, L.J., Höhfeld, J., and Patterson, C. (2001). The co-chaperone CHIP regulates protein triage decisions mediated by heat-shock proteins. *Nat. Cell Biol.* 3, 93–96.
- Das, A.K., Cohen, P.W., and Barford, D. (1998). The structure of the tetratrico-peptide repeats of protein phosphatase 5: implications for TPR-mediated protein-protein interactions. *EMBO J.* 17, 1192–1199.
- DeLano, W.L. (2010). The PyMOL molecular graphics system, version 1.3r1. In The PyMOL Molecular Graphics System, Version 1.3r1The PyMOL Molecular Graphics System, Version 1.3r1 (New York: Schrödinger).
- Diebold, M.L., Fribourg, S., Koch, M., Metzger, T., and Romier, C. (2011). Deciphering correct strategies for multiprotein complex assembly by co-expression: application to complexes as large as the histone octamer. *J. Struct. Biol.* 175, 178–188.

- Eckert, K., Saliou, J.M., Monlezun, L., Vigouroux, A., Atmane, N., Caillat, C., Quevillon-Chéruel, S., Madiona, K., Nicaise, M., Lazereg, S., et al. (2010). The Pih1-Tah1 cochaperone complex inhibits Hsp90 molecular chaperone ATPase activity. *J. Biol. Chem.* 285, 31304–31312.
- Finn, R.D., Mistry, J., Tate, J., Coggill, P., Heger, A., Pollington, J.E., Gavin, O.L., Gunasekaran, P., Ceric, G., Forslund, K., et al. (2010). The Pfam protein families database. *Nucleic Acids Res.* 38(Database issue), D211–D222.
- Goddard, T.D., and Kneller, D.G. (2002). SPARKY 3 (San Francisco: University of California).
- Gonzales, F.A., Zanchin, N.I., Luz, J.S., and Oliveira, C.C. (2005). Characterization of *Saccharomyces cerevisiae* Nop17p, a novel Nop58p-interacting protein that is involved in Pre-rRNA processing. *J. Mol. Biol.* 346, 437–455.
- Güntert, P. (2004). Automated NMR structure calculation with CYANA. *Methods Mol. Biol.* 278, 353–378.
- Herrmann, T., Güntert, P., and Wüthrich, K. (2002a). Protein NMR structure determination with automated NOE-identification in the NOESY spectra using the new software ATNOS. *J. Biomol. NMR* 24, 171–189.
- Herrmann, T., Güntert, P., and Wüthrich, K. (2002b). Protein NMR structure determination with automated NOE assignment using the new software CANDID and the torsion angle dynamics algorithm DYANA. *J. Mol. Biol.* 319, 209–227.
- Horejši, Z., Takai, H., Adelman, C.A., Collis, S.J., Flynn, H., Maslen, S., Skehel, J.M., de Lange, T., and Boulton, S.J. (2010). CK2 phospho-dependent binding of R2TP complex to TEL2 is essential for mTOR and SMG1 stability. *Mol. Cell* 39, 839–850.
- Jiménez, B., Ugwu, F., Zhao, R., Ortí, L., Makhnevych, T., Pineda-Lucena, A., and Houry, W.A. (2012). Structure of minimal tetratricopeptide repeat domain protein Tah1 reveals mechanism of its interaction with Pih1 and Hsp90. *J. Biol. Chem.* 287, 5698–5709.
- Koradi, R., Billeter, M., and Wuthrich, K. (1996). MOLMOL: a program for display and analysis of macromolecular structures. *J. Mol. Graph.* 14, 29–32, 51–55.
- Laskowski, R.A., Rullmann, J.A., MacArthur, M.W., Kaptein, R., and Thornton, J.M. (1996). AQUA and PROCHECK-NMR: programs for checking the quality of protein structures solved by NMR. *J. Biomol. NMR* 8, 477–486.
- Li, J., Qian, X., Hu, J., and Sha, B. (2009). Molecular chaperone Hsp70/Hsp90 prepares the mitochondrial outer membrane translocon receptor Tom70 for preprotein loading. *J. Biol. Chem.* 284, 23852–23859.
- Li, J., Soroka, J., and Buchner, J. (2012). The Hsp90 chaperone machinery: conformational dynamics and regulation by co-chaperones. *Biochim. Biophys. Acta* 1823, 624–635.
- Meyer, E.A., Castellano, R.K., and Diederich, F. (2003a). Interactions with aromatic rings in chemical and biological recognition. *Angew. Chem. Int. Ed. Engl.* 42, 1210–1250.
- Meyer, P., Prodromou, C., Hu, B., Vaughan, C., Roe, S.M., Panaretou, B., Piper, P.W., and Pearl, L.H. (2003b). Structural and functional analysis of the middle segment of hsp90: implications for ATP hydrolysis and client protein and cochaperone interactions. *Mol. Cell* 11, 647–658.
- Millson, S.H., Vaughan, C.K., Zhai, C., Ali, M.M., Panaretou, B., Piper, P.W., Pearl, L.H., and Prodromou, C. (2008). Chaperone ligand-discrimination by the TPR-domain protein Tah1. *Biochem. J.* 413, 261–268.
- Nelson, G.M., Huffman, H., and Smith, D.F. (2003). Comparison of the carboxy-terminal DP-repeat region in the co-chaperones Hop and Hip. *Cell Stress Chaperones* 8, 125–133.
- Paci, A., Liu, X.H., Huang, H., Lim, A., Houry, W.A., and Zhao, R. (2012). The stability of the small nucleolar ribonucleoprotein (snoRNP) assembly protein Pih1 in *Saccharomyces cerevisiae* is modulated by its C terminus. *J. Biol. Chem.* 287, 43205–43214.
- Pearl, L.H., and Prodromou, C. (2006). Structure and mechanism of the Hsp90 molecular chaperone machinery. *Annu. Rev. Biochem.* 75, 271–294.
- Prodromou, C. (2012). The ‘active life’ of Hsp90 complexes. *Biochim. Biophys. Acta* 1823, 614–623.
- Russell, L.C., Whitt, S.R., Chen, M.S., and Chinkers, M. (1999). Identification of conserved residues required for the binding of a tetratricopeptide repeat domain to heat shock protein 90. *J. Biol. Chem.* 274, 20060–20063.
- Sattler, M., Schleucher, J., and Griesinger, C. (1999). Heteronuclear multi-dimensional NMR experiments for the structure determination of proteins in solution employing pulsed field gradients. *Prog. Nucl. Magn. Reson. Spectrosc.* 34, 93–158.
- Scheufler, C., Brinker, A., Bourenkov, G., Pegoraro, S., Moroder, L., Bartunik, H., Hartl, F.U., and Moarefi, I. (2000). Structure of TPR domain-peptide complexes: critical elements in the assembly of the Hsp70-Hsp90 multichaperone machine. *Cell* 101, 199–210.
- Schmid, A.B., Lagleder, S., Gräwert, M.A., Röhl, A., Hagn, F., Wandinger, S.K., Cox, M.B., Demmer, O., Richter, K., Groll, M., et al. (2012). The architecture of functional modules in the Hsp90 co-chaperone Sti1/Hop. *EMBO J.* 31, 1506–1517.
- Theodoraki, M.A., and Caplan, A.J. (2012). Quality control and fate determination of Hsp90 client proteins. *Biochim. Biophys. Acta* 1823, 683–688.
- Whitesell, L., and Cook, P. (1996). Stable and specific binding of heat shock protein 90 by geldanamycin disrupts glucocorticoid receptor function in intact cells. *Mol. Endocrinol.* 10, 705–712.
- Whitesell, L., and Lin, N.U. (2012). HSP90 as a platform for the assembly of more effective cancer chemotherapy. *Biochim. Biophys. Acta* 1823, 756–766.
- Zeytuni, N., and Zarivach, R. (2012). Structural and functional discussion of the tetra-trico-peptide repeat, a protein interaction module. *Structure* 20, 397–405.
- Zhang, M., Windheim, M., Roe, S.M., Peggie, M., Cohen, P., Prodromou, C., and Pearl, L.H. (2005). Chaperoned ubiquitylation—crystal structures of the CHIP U box E3 ubiquitin ligase and a CHIP-Ubc13-Uev1a complex. *Mol. Cell* 20, 525–538.
- Zhao, R., Davey, M., Hsu, Y.C., Kaplanek, P., Tong, A., Parsons, A.B., Krogan, N., Cagney, G., Mai, D., Greenblatt, J., et al. (2005). Navigating the chaperone network: an integrative map of physical and genetic interactions mediated by the hsp90 chaperone. *Cell* 120, 715–727.
- Zhao, R., Kakihara, Y., Gribun, A., Huen, J., Yang, G., Khanna, M., Costanzo, M., Brost, R.L., Boone, C., Hughes, T.R., et al. (2008). Molecular chaperone Hsp90 stabilizes Pih1/Nop17 to maintain R2TP complex activity that regulates snoRNA accumulation. *J. Cell Biol.* 180, 563–578.